Molecular Genomic Profiling of Melanocytic Nevi

Andrew J. Colebatch[1,2], Peter Ferguson[1,2], Felicity Newell[3], Stephen H. Kazakoff[3], Tom Witkowski[4], Alexander Dobrovic[4,5,6], Peter A. Johansson[3], Robyn P.M. Saw[1,7,8], Jonathan R. Stretch[1,7], Grant A. McArthur[9,10], Georgina V. Long[1,7,11], John F. Thompson[1,7,8], John V. Pearson[3,13], Graham J. Mann[1,7,12,13], Nicholas K. Hayward[3,13], Nicola Waddell[3,13], Richard A. Scolyer[1,2,7,13] and James S. Wilmott[1,7,13]

The benign melanocytic nevus is the most common tumor in humans and rarely transforms into cutaneous melanoma. Elucidation of the nevus genome is required to better understand the molecular steps of progression to melanoma. We performed whole genome sequencing on a series of 14 benign melanocytic nevi consisting of both congenital and acquired types. All nevi had driver mutations in the MAPK signaling pathway, either *BRAF* V600E or *NRAS* Q61R/L. No additional definite driver mutations were identified. Somatic mutations in nevi with higher mutation loads showed a predominance of mutational signatures 7a and 7b, consistent with UVR exposure, whereas nevi with lower mutation loads (including all three congenital nevi) had a predominance of the ubiquitous signatures 1 and 5. Two nevi had mutations in promoter regions predicted to bind E26 transformation-specific family transcription factors, as well as subclonal mutations in the *TERT* promoter. This paper presents whole genome data from melanocytic nevi. We confirm that UVR is involved in the etiology of a subset of nevi. This study also establishes that *TERT* promoter mutations are present in morphologically benign skin nevi in subclonal populations, which has implications regarding the interpretation of this emerging biomarker in sensitive assays.

Journal of Investigative Dermatology (2019) **139,** 1762–1768; doi:10.1016/j.jid.2018.12.033

INTRODUCTION

The melanocytic nevus, the commonest tumor occurring in humans, is a benign proliferation of melanocytes, which typically arises in the skin. Melanocytic nevi that are present at birth are designated as congenital nevi, while those arising after birth are termed acquired nevi. Although melanocytic nevi are considered biologically benign, a small proportion (annual rate of between <1 in 200,000 to 1 in 33,000 (Tsao et al., 2003) transform to melanoma. Approximately 30% of melanomas arise within or adjacent to a pre-existing nevus (Lin et al., 2015; Pampena et al., 2017), with genomic analysis confirming the clonal origin of melanomas from adjacent nevi (Shain et al., 2015b). As such, further genomic analysis of nevi is required to potentially elucidate the mechanisms that lead to transformation of a nevus to melanoma in a small but clinically significant subset of cases.

Recent studies have demonstrated the frequent occurrence of noncoding driver mutations in cutaneous melanoma, including *TERT* promoter mutations (Horn et al., 2013; Huang et al., 2013), as well as other noncoding mutations occurring within promoters (Fredriksson et al., 2014; Melton et al., 2015; Weinhold et al., 2014). *TERT* promoter mutations are present in approximately 80% of cutaneous melanomas (The Cancer Genome Atlas Network, 2015; Griewank et al., 2014; Hayward et al., 2017; Heidenreich et al., 2014) and are C→T transitions, occurring most commonly at one of two positions: chr5:1295228 or chr5:1295250, within the core promoter region. *TERT* promoter mutations create novel E26 transformation-specific transcription factor binding sites (Bell et al., 2015; Horn et al., 2013; Huang et al., 2013), and promote melanoma cell survival and immortalization through increased telomerase activity, although in a manner that does not prevent telomere shortening (Chiba et al., 2017).

TERT promoter mutations have not been detected in benign nevi (Horn et al., 2013; Shain et al., 2015b; Stark et al., 2018; Vinagre et al., 2013), suggesting that these mutations might be a useful biomarker of malignancy in

[1]*Melanoma Institute Australia, The University of Sydney, New South Wales, Australia;* [2]*Tissue Pathology and Diagnostic Oncology, Royal Prince Alfred Hospital, Camperdown, New South Wales, Australia;* [3]*Queensland Institute of Medical Research, Berghofer Medical Research Institute, Brisbane, Queensland, Australia;* [4]*Olivia Newton-John Cancer Research Institute, Heidelberg, Victoria, Australia;* [5]*School of Cancer Medicine and Molecular Cancer Prevention Program, La Trobe University, Bundoora, Victoria, Australia;* [6]*Department of Clinical Pathology, University of Melbourne, Parkville, Victoria, Australia;* [7]*Sydney Medical School, The University of Sydney, Sydney, New South Wales, Australia;* [8]*Department of Melanoma and Surgical Oncology, Discipline of Surgery, Royal Prince Alfred Hospital, Sydney, New South Wales, Australia;* [9]*Peter MacCallum Cancer Centre, East Melbourne, Victoria, Australia;* [10]*Sir Peter MacCallum Department of Oncology, University of Melbourne, Parkville, Victoria, Australia;* [11]*Royal North Shore Hospital, Sydney, New South Wales, Australia; and* [12]*Centre for Cancer Research, Westmead Institute for Medical Research, The University of Sydney, Westmead, New South Wales, Australia*

[13]*These authors contributed equally to this work.*

Correspondence: Andrew J. Colebatch, Tissue Pathology and Diagnostic Oncology, Royal Prince Alfred Hospital, Camperdown, New South Wales, Australia 2050. E-mail: Andrew.colebatch@health.nsw.gov.au

Abbreviations: ddPCR, droplet digital PCR; WGS, whole genome sequencing

Received 16 October 2018; revised 4 December 2018; accepted 5 December 2018; accepted manuscript published online 14 February 2019; corrected proof published online 18 April 2019

melanocytic neoplasms. However, the genomic evaluation of melanocytic precursor lesions adjacent to melanoma indicates relatively early acquisition of *TERT* promoter mutations during progression from nevus to melanoma (Shain et al., 2015b, 2018). In these two studies by Shain et al. (2015b, 2018) melanocytic lesions with morphologic characteristics intermediate between benign nevi and melanomas, corresponding to the nosological entities of dysplastic nevi or melanocytomas, demonstrated *TERT* promoter mutations.

In light of the possible significance of noncoding mutations in melanocytic tumor pathogenesis, we sought to comprehensively analyze the entire genomes of a set of benign melanocytic nevi, as well as to evaluate *TERT* promoter mutation status with maximum sensitivity (since the *TERT* promoter region is poorly covered by whole genome sequencing [WGS]). Although exome sequencing studies of nevi have been performed (Melamed et al., 2017; Stark et al., 2018), to the best of our knowledge, no WGS analysis of cutaneous nevi has been performed to date.

RESULTS AND DISCUSSION

Single nucleotide variants in nevus genomes

We performed WGS of 14 benign melanocytic nevi, of which 3 were congenital and 11 were acquired (Table 1). There were no dysplastic nevi in our study group. The WGS of nevi achieved a mean coverage of 50× (range 45−55×), and of blood samples achieved a mean coverage of 34× (range 28−40×). The total number of somatic single nucleotide variants in the nevus genomes ranged from 181 to 38,437 (median 665) or from 0.1 to 12.2 mutations per megabase. The total number of nonsynonymous mutations varied between 1 and 185 (median 4.5) per sample. The median nonsynonymous mutation load of this set is lower than previously published exome data sets of acquired nevi, with an intermediate range: Stark et al. (2018) found deleterious mutation loads of 13−340 (median 89) in cases that were a mix of benign and dysplastic nevi, and Melamed et al. (2017) found a range of 0−46 (median 19) in a set of 19 dysplastic nevi. The low or intermediate loads we identified in comparison to the other published sets are likely to be the result of decreased UV light exposure in our cohort and also the inclusion of congenital nevi and absence of dysplastic nevi.

The mean coverage of 50× in this study is sufficient to detect mutations fixed early in nevogenesis. However, this depth of sequencing coverage will not be able to detect somatic mutations arising within potential subclones at low allelic fractions.

Driver mutations and noncoding mutations in nevi

All sequenced nevi had activation of the MAPK pathway, with mutually exclusive mutations in either *BRAF* or *NRAS*: four nevi had *NRAS* mutations (three Q61R and one Q61K) and the remainder (n = 11) had *BRAF* V600E mutations. All three congenital nevi had *NRAS* mutations, consistent with prior reports (Bauer et al., 2007; Lu et al., 2015; Melamed et al., 2017).

No other genes were recurrently mutated among the nevus samples. A collated list of putative driver mutations in melanoma (Zhang et al., 2016) was used to assess possible candidate driver mutations in nevi. Nevus case 13, an acquired dermal nevus occurring in a 59-year-old male, was the sample with the highest single nucleotide variant load and had a mutation at the *NFKBIE* hotspot (chr6:44233400) previously described in desmoplastic melanoma (Shain et al., 2015a). No other putative driver mutations were identified.

Previously annotated promoter mutations were evaluated in the nevi. These mutations occur in motifs within active promoters that match E26 transformation-specific transcription factor binding sites and are recurrently mutated in approximately 80% of cutaneous melanomas (Colebatch et al., 2016). In nevus case 11, an acquired compound nevus occurring in a 50-year-old female, promoter mutations were present in *SMUG1* and *RPL13A*; in nevus case 13, promoter mutations were present in *C16orf91* and *ARHGEF18*. No other promoter mutations were present. Recent work has demonstrated that promoter mutations at E26 transformation-specific transcription factor binding sites are a unique signature of UVR that correlate with overall mutation burden (Fredriksson et al., 2017; Mao et al., 2018). These mutations result from increased susceptability for cyclobutane pyrimidine dimer formation due to conformational changes induced in DNA by E26 transformation-specific binding, rather than decreased DNA repair at these sites (Mao et al., 2018).

Mutational signatures in nevi

Recent large-scale genomics studies performed on a range of different cancer types have revealed multiple mutational signatures, many of which can be attributed to specific etiologic factors, such as carcinogens or DNA repair defects that are implicated in the pathogenesis of the tumor (Alexandrov et al., 2013). However, there is only very limited information currently available on mutational signatures in nevi and what exists is based on whole exome sequencing data (i.e., analyzing approximately 1% of the human genome).

Our WGS study provided an opportunity to gain more in-depth insights into mutagenic processes important in the pathogenesis of nevi. There are currently 30 curated mutation signatures, defined as the base substitution frequency of each possible single nucleotide variant in the context of 3′ and 5′ flanking bases (yielding a matrix of 96 non-redundant substitutions). Signature 7 was detected in most nevi, accounting for up to 90% of the mutations identified (Figure 1). Signature 7 is dominated by C→T mutations located at dipyrimidine sites, and has been shown to be generated by UVR in vitro (Nik-Zainal et al., 2015). Signature 7 is also the dominant mutation signature present in cutaneous melanoma (Hayward et al., 2017) and has been found in acquired melanocytic nevi in a study analyzing exome sequence data (Stark et al., 2018).

A previous WGS study of melanoma further divided signature 7 into three signatures: 7a, 7b, and 7c, (Hayward et al., 2017). Based on the particular base pair substitutions and flanking bases, signature 7a is proposed to be due to 6,4-photoproducts, signature 7b due to cyclobutane pyrimidine dimers, and signature 7c due to indirect DNA damage after UVR. Analysis of the nevi using the subdivided signature 7 demonstrates that the highly mutated nevi are dominated by

Table 1. Clinical, pathologic and genetic features of 14 nevi

Case	Age at excision, y	Sex	Site	Size, mm	Congenital/ acquired	Architectural growth pattern	BRAF/ NRAS	Deleterious mutations, n	Donor ID
Nevus 1	56	Male	Chin	NA	Acquired	Dermal	BRAF V600E	61	MELA_0775
Nevus 2	15	Male	Thigh	35	Congenital	Dermal	NRAS Q61R	1	MELA_0769
Nevus 3	16	Female	Shoulder	30	Congenital	Compound	NRAS Q61R	1	MELA_0770
Nevus 4	44	Male	Cheek	8	Acquired	Dermal	NRAS Q61R	15	MELA_0776
Nevus 5	56	Male	NA	NA	Acquired	Dermal	BRAF V600E	4	MELA_0778
Nevus 6	27	Male	Neck	8	Acquired	Compound	BRAF V600E	56	MELA_0772
Nevus 7	39	Male	Jaw	NA	Acquired	Compound	BRAF V600E	4	MELA_0781
Nevus 8	42	Female	Chin	3	Acquired	Compound	BRAF V600E	7	MELA_0782
Nevus 9	11	Male	Chin	28	Congenital	Compound	NRAS Q61L	2	MELA_0773
Nevus 10	36	Female	Jaw	NA	Acquired	Dermal	BRAF V600E	2	MELA_0783
Nevus 11	50	Female	Temple	6	Acquired	Compound	BRAF V600E	117	MELA_0784
Nevus 12	46	Female	Face	NA	Acquired	Dermal	BRAF V600E	4	MELA_0785
Nevus 13	59	Male	Face	NA	Acquired	Dermal	BRAF V600E	185	MELA_0786
Nevus 14	31	Female	Cheek	7	Acquired	Dermal	BRAF V600E	5	MELA_0787

Abbreviation: NA, not applicable.

signatures 7a and 7b, with signature 7c in the three nevi with the highest mutation burdens (Figure 1), similar to the pattern identified in cutaneous melanoma (Hayward et al., 2017).

Signatures 1 and 5 were elevated in tumors without evidence of signature 7, including the three congenital nevi. Signature 1 is related to spontaneous deamination of 5-methylcytosine and correlates with age. In contrast, the etiology behind signature 5 is currently unknown. From this study, there are two categories of nevi as distinguished by the mutational signatures observed in the genome: a UVR-high group defined by contributions of signatures 7a, 7b, and 7c, and a UVR-low group defined by signatures 1 and 5; the latter group includes congenital nevi. The UVR-high category, present in those nevi with elevated mutation loads, implies either that there is acquisition of additional mutations in nevi over time after they have initially formed, or that nevi arise from a highly mutated skin-resident melanocyte precursor cell. The former proposal contrasts with a model of nevi as cell cycle arrested senescent proliferations (Michaloglou et al., 2005).

TERT promoter mutations in nevi

DNA was available from 13 nevi for analysis of the two common *TERT* promoter mutations using droplet digital PCR (ddPCR). Two nevi had detectable *TERT* promoter mutations: case 13, an acquired dermal nevus in a 59-year-old male, had a C250T mutation at 0.2% allele fraction (Figure 2), and case 11, an acquired compound nevus in a 50-year-old female had both a C228T mutation at 0.2% allelic fraction and a C250T mutation at 0.2% allelic fraction (Tables 2 and 3). Sanger sequencing of the *TERT* promoter region of all 14 samples failed to demonstrate mutations (data not shown). This study includes the demonstration of *TERT* promoter mutations in unequivocally benign nevi, which is, to our knowledge, previously unreported. Previous studies of *TERT* promoter mutations in benign nevi did not demonstrate either of the two common *TERT* promoter mutations (Horn et al., 2013; Shain et al., 2015b; Stark et al., 2018; Vinagre et al., 2013), while *TERT* promoter mutations were identified in "intermediate" melanocytic lesions (corresponding to dysplastic nevi) (Shain et al., 2015b). One reason for the difference of our results with previous studies is due to the much higher sensitivity of the ddPCR technique we utilized (Colebatch et al., 2018) compared with the lower sensitivity of prior experimental techniques, such as Sanger sequencing or custom capture sequencing panels. ddPCR for *TERT* promoter mutations can detect mutant alleles down to an allele fraction of approximately 0.02% (Colebatch et al., 2018), indicating that the identified promoter mutation in the two

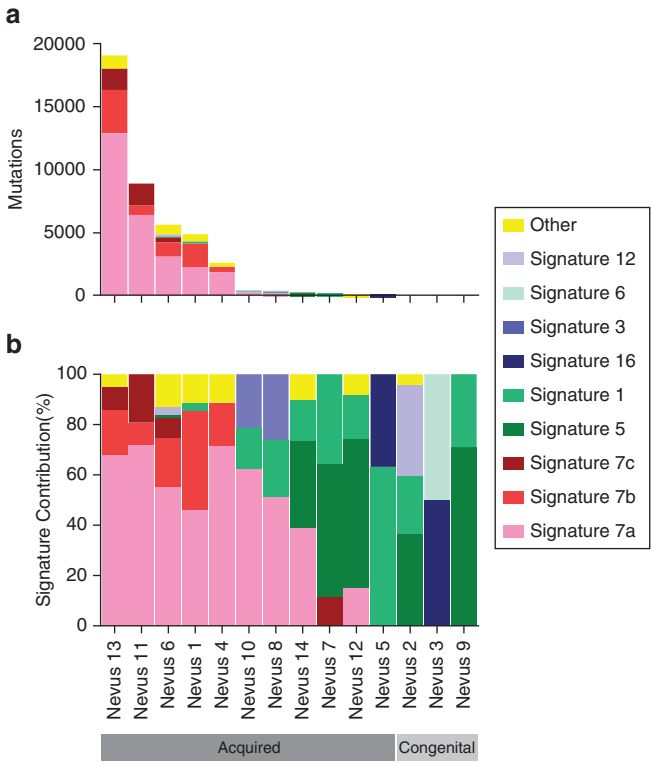

Figure 1. Nevus genome mutational signatures. (**a**) Absolute contribution of mutational signatures to overall single nucleotide variant count for each nevus. (**b**) Relative contribution of mutational signatures to total overall single nucleotide variant count for each nevus.

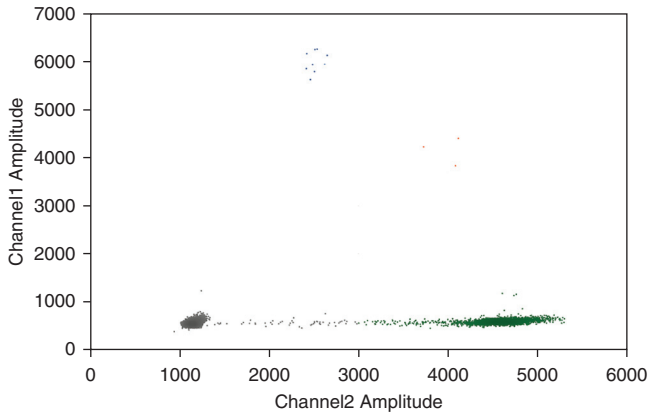

Figure 2. Example of droplet digital PCR droplets for *TERT* C250T and C250C in nevus 13. Blue droplets are classified as mutant only, green droplets as wild-type only, and orange droplets as double-mutant wild-type combined droplets.

nevi are within the detection limits of the assay. Similar identification of *TERT* promoter mutations is already being utilized in some clinical pathology laboratories as a diagnostic adjunct test to assist in distinguishing melanomas from nevi, due to the presence of these mutations in the former and absence in the latter. The detection of *TERT* promoter mutations in benign lesions in our study, therefore, has implications for sensitive assays that may utilize this mutation as a biomarker of malignancy, in that low levels may be compatible with benign lesions.

There are two potential explanations for the apparent presence of *TERT* promoter mutations in a small proportion of benign nevi. The first is that minor subclones with *TERT* promoter mutations may be present in certain nevi, and these may be part of the mechanism of transformation of benign nevi to melanoma, representing an early focus of transformation that cannot be demonstrated by current morphologic analysis. The presence of such subclones would be consistent with the presence of ongoing mutations in nevi, as discussed in "UVR-high" nevi. The second possibility is that the *TERT* promoter mutant subclones are contaminants from adjacent keratinocytes. Somatic mutations are present in sun-exposed, morphologically normal skin (Martincorena and Campbell, 2015), although *TERT* has not been examined to date. The two nevi with *TERT* promoter mutations show evidence of prolonged UVR exposure, with a large contribution of signature 7 to the mutation profile of both. Moreover, the presence of promoter mutations at E26 transformation-specific binding sites in both samples is consistent with prior chronic UV irradiation (Colebatch et al., 2016; Fredriksson et al., 2017). As such, the adjacent skin would

Table 2. Droplet digital PCR results of *TERT* C228T mutation in 13 nevi

Case no.	Target	Total droplets, n	Positive droplets, n	Negative droplets, n	cpm	*P*-value[1]
Nevus 1	TERT C228T mut	15,075	3	15,072	0.23	0.11
Nevus 1	TERT C228C wt	15,075	7,778	7,297	853.62	—
Nevus 2	TERT C228T mut	14,411	1	14,410	0.08	0.641
Nevus 2	TERT C228C wt	14,411	8,239	6,172	997.61	—
Nevus 3	TERT C228T mut	14,597	2	14,595	0.16	0.292
Nevus 3	TERT C228C wt	14,597	3,712	10,885	345.21	—
Nevus 5	TERT C228T mut	14,546	1	14,545	0.08	0.644
Nevus 5	TERT C228C wt	14,546	6,362	8,184	676.63	—
Nevus 6	TERT C228T mut	15,720	1	15,719	0.07	0.672
Nevus 6	TERT C228C wt	15,720	3,914	11,806	336.85	—
Nevus 7	TERT C228T mut	16,328	1	16,327	0.07	0.685
Nevus 7	TERT C228C wt	16,328	6,448	9,880	591.02	—
Nevus 8	TERT C228T mut	15,212	1	15,211	0.08	0.66
Nevus 8	TERT C228C wt	15,212	6,268	8,944	624.83	—
Nevus 9	TERT C228T mut	15,176	0	15,176	0	1
Nevus 9	TERT C228C wt	15,176	6,128	9,048	608.44	—
Nevus 10	TERT C228T mut	15,079	1	15,078	0.08	0.657
Nevus 10	TERT C228C wt	15,079	6,420	8,659	652.59	—
Nevus 11	TERT C228T mut	17,348	131	17,217	8.92	**<0.001**
Nevus 11	TERT C228C wt	17,348	16,804	544	4,073.27	—
Nevus 12	TERT C228T mut	30,812	3	30,809	0.11	0.392
Nevus 12	TERT C228C wt	30,812	15,577	15,235	828.6	—
Nevus 14	TERT C228T mut	15,764	0	15,764	0	1
Nevus 14	TERT C228C wt	15,764	3,505	12,259	295.85	—
Nevus 13	TERT C228T mut	14,954	0	14,954	0	1
Nevus 13	TERT C228C wt	14,954	4,128	10,826	380.03	—
SK-MEL28[2]	TERT C228T mut	175,734	12	175,722	0.08	NA
SK-MEL28[2]	TERT C228C wt	175,734	65,709	110,025	550.9	—

Abbreviations: cpm, copies per microliter; mut, mutant probe; wt, wild-type probe.
[1]Result of Fisher's exact test comparing mutant droplets to wild-type controls.
[2]SK-MEL28 is the wild-type control.

Table 3. Droplet digital PCR results of *TERT* C250T mutation in 13 nevi

Case no.	Target	Total droplets	Positive droplets	Negative droplets	cpm	*P*-value[1]
Nevus 1	TERT C250T mut	12,777	2	12,775	0.18	0.311
Nevus 1	TERT C250C wt	12,777	6,179	6,598	777.51	—
Nevus 2	TERT C250T mut	14,036	3	14,033	0.25	0.144
Nevus 2	TERT C250C wt	14,036	7,769	6,267	948.62	—
Nevus 3	TERT C250T mut	15,120	1	15,119	0.08	0.709
Nevus 3	TERT C250C wt	15,120	3,929	11,191	354.01	—
Nevus 5	TERT C250T mut	13,166	4	13,162	0.36	0.043
Nevus 5	TERT C250C wt	13,166	5,903	7,263	699.82	—
Nevus 6	TERT C250T mut	15,393	0	15,393	0	1
Nevus 6	TERT C250C wt	15,393	3,899	11,494	343.63	—
Nevus 7	TERT C250T mut	15,862	0	15,862	0	1
Nevus 7	TERT C250C wt	15,862	5,654	10,208	518.53	—
Nevus 8	TERT C250T mut	12,998	0	12,998	0	1
Nevus 8	TERT C250C wt	12,998	5,975	7,023	724.24	—
Nevus 9	TERT C250T mut	14,947	0	14,947	0	1
Nevus 9	TERT C250C wt	14,947	5,488	9,459	538.29	—
Nevus 10	TERT C250T mut	13,453	1	13,452	0.09	0.669
Nevus 10	TERT C250C wt	13,453	5,680	7,773	645.35	—
Nevus 11	TERT C250T mut	15,349	13	15,336	1	**<0.001**
Nevus 11	TERT C250C wt	15,349	4,695	10,654	429.55	—
Nevus 12	TERT C250T mut	15,596	2	15,594	0.15	0.392
Nevus 12	TERT C250C wt	15,596	7,743	7,853	807.2	—
Nevus 14	TERT C250T mut	16,287	1	16,286	0.07	0.733
Nevus 14	TERT C250C wt	16,287	3,546	12,741	288.87	—
Nevus 13	TERT C250T mut	15,969	12	15,957	0.88	**<0.001**
Nevus 13	TERT C250C wt	15,969	4,433	11,536	382.56	—
SK-MEL28[2]	TERT C250T mut	78,524	6	78,518	0.09	NA
SK-MEL28[2]	TERT C250C wt	78,524	28,812	49,712	537.83	—

Abbreviations: cpm, copies per microliter; mut, mutant probe; NA, not applicable; wt, wild-type probe.
[1]Result of Fisher's exact test comparing mutant droplets to wild-type controls.
[2]SK-MEL28 is the wild-type control.

be expected to harbor high mutation loads, which may include *TERT* promoter mutations. Further experiments are required to evaluate the existence of *TERT* promoter mutations in sun-exposed skin.

Our study presents WGS analysis of benign cutaneous nevi and demonstrates that while their mutation load was generally very low, they all carried mutually exclusive driver mutations in MAPK oncogenes *BRAF* and *NRAS*. Mutation signature analysis defined two subclasses of nevi, one demonstrating a predominant UVR signature (signatures 7a, 7b, and 7c) and the other, which includes congenital nevi, lacking a UVR signature and driven by signatures 1 and 5. These findings substantially validate the results of prior studies that have investigated the mutational landscape of nevi. Furthermore, utilizing a highly sensitive ddPCR assay, *TERT* promoter mutations may occasionally be detected in acquired nevi, which has important implications for interpretation of *TERT* promoter assays being used as diagnostic adjunct testing in clinical practice for the diagnosis of histologically challenging melanocytic tumors.

MATERIALS AND METHODS

Patient cohort

Eighteen nevi from 18 patients were recruited for this study and all were lesions that were clinically longstanding, showed no clinical features suspicious for melanoma, and were excised for cosmetic reasons at the request of the patient. Following written informed consent, a portion (usually approximately 50%) of the nevus was fresh-frozen for genomic analysis. The remainder of the tumor was processed and evaluated routinely by conventional histopathology.

Human nevus samples

The fresh-frozen tissue and blood samples analyzed in the current study were obtained from The Melanoma Institute Australia biospecimen bank with written informed patient consent and Institutional Review Board approval (The Sydney Local Health District Human Research Ethics Committee, Protocol No. X15-0454 and HREC/11/RPAH/444). Cases were selected based on clinical and pathological confirmation of a diagnosis of a benign nevus. Congenital nevi were diagnosed when there was a documented history that they were present at birth.

Of the 18 nevi obtained for analysis, 2 cases were excluded due to having *BRAF* mutation allele fractions <5% by ddPCR, while 2 other cases had <100 single nucleotide variants and >40% of somatic calls matching dbSNP entries, indicating low tumor content.

DNA extractions and whole genome sequencing

Tumor DNA for WGS was extracted from fresh-frozen tissue using DNeasy Blood and Tissue Kits (69506; Qiagen). Whole blood DNA

for WGS was extracted using Flexigene DNA Kits (51206; Qiagen) as described previously (Wilmott et al., 2015). WGS was performed on a HiseqX10 instrument (Illumina, San Diego, CA) as described (Hayward et al., 2017). Somatic mutation calling was performed as described (Hayward et al., 2017). The BAM files have been deposited in the European Genome-phenome Archive (https://www.ebi.ac.uk/ega/) with accession number EGAS00001001552.

Signature analysis

Decomposition of mutational signatures was performed using the *deconstructSigs* and *MutationalPatterns* packages for R, version 3.4.2. The set of 30 Catalogue of Somatic Mutations in Cancer mutational signatures was obtained from http://cancer.sanger.ac.uk/cancergenome/assets/signatures_probabilities.txt. Mutational signatures for 7a, 7b, and 7c were extracted from a larger whole genome analysis of cutaneous melanomas (Hayward et al., 2017).

ddPCR

ddPCR was performed on a QX200 Droplet Digital PCR System (Bio-Rad, Hercules, CA). Droplet generation was performed using an AutoDG (Bio-Rad) droplet generator. The PCR step was performed on a C1000 Touch Thermal Cycler (Bio-Rad). After the PCR step, the sealed plate was loaded onto a QX200 Droplet Reader in order to analyze the droplet fluorescent intensity. Initial data analysis was performed using the Quantasoft Pro software suite, version 1.0 (Bio-Rad) in order to evaluate the droplet quality and establish manual thresholds.

The ddPCR analysis of *BRAF* V600E was performed according to the method described by Tsao et al. (2015), whereas for *TERT* C228T and C250T ddPCR followed the method described by Colebatch et al. (2018).

Statistics

For the analysis of mutant droplets in nevi, a Fisher's exact test was performed comparing these to false-positive droplets from the pooled wild-type samples (SK-MEL28). A *P*-value of <0.01 was considered significant. Statistical testing was performed in R, version 3.2.0.

ORCID

Andrew J. Colebatch: http://orcid.org/0000-0002-7610-3984

CONFLICTS OF INTEREST

Alexander Dobrovic: honoraria from Bio-Rad for speaking (not directly related to this paper). Grant A. McArthur: principal investigator of clinical trials with Genentech/Roche, MSD, BMS, Array BioPharm, Amgen, Pfizer (all revenues paid to institution as reimbursement for trial costs). John F. Thompson: Advisory board membership and honoraria from BMS Australia, GlaxoSmithKline, MSD Australia, and Provectus. The remaining authors state no conflict of interest.

ACKNOWLEDGMENTS

This work was supported by Melanoma Institute Australia, Bioplatforms Australia, New South Wales Ministry of Health, Cancer Council New South Wales, Program Grants of the National Health and Medical Research Council of Australia, Cancer Institute New South Wales, and by the Australian Cancer Research Foundation. NW, JSW, NKH, GVL, and RAS are supported by National Health and Medical Research Council of Australia Fellowships. The authors gratefully acknowledge the support of colleagues at Melanoma Institute Australia, Royal Prince Alfred Hospital, NSW Health Pathology, the Westmead Institute for Medical Research. PF was supported by the Deborah and John McMurtrie Melanoma Institute Australia Pathology Fellowship. Andrew Colebatch is a recipient of the Postgraduate Research Fellowship 2015 from the Royal College of Pathologists of Australasia Foundation. The Olivia Newton-John Cancer Research Institute received support from the Operational Infrastructure Support Program of the Victorian State Government. GVL is supported by a University of Sydney, Sydney Medical School Foundation Grant.

REFERENCES

Alexandrov LB, Nik-Zainal S, Wedge DC, Aparicio SA, Behjati S, Biankin AV, et al. Signatures of mutational processes in human cancer. Nature 2013;500(7463):415–21.

Bauer J, Curtin JA, Pinkel D, Bastian BC. Congenital melanocytic nevi frequently harbor NRAS mutations but no BRAF mutations. J Invest Dermatol 2007;127:179–82.

Bell RJ, Rube HT, Kreig A, Mancini A, Fouse SD, Nagarajan RP, et al. Cancer. The transcription factor GABP selectively binds and activates the mutant TERT promoter in cancer. Science 2015;348(6238):1036–9.

Chiba K, Lorbeer FK, Shain AH, McSwiggen DT, Schruf E, Oh A, et al. Mutations in the promoter of the telomerase gene TERT contribute to tumorigenesis by a two-step mechanism. Science 2017;357(6358):1416–20.

Colebatch AJ, Di Stefano L, Wong SQ, Hannan RD, Waring PM, Dobrovic A, et al. Clustered somatic mutations are frequent in transcription factor binding motifs within proximal promoter regions in melanoma and other cutaneous malignancies. Oncotarget 2016;7:66569–85.

Colebatch AJ, Witkowski T, Waring PM, McArthur GA, Wong SQ, Dobrovic A. Optimizing amplification of the GC-rich TERT promoter region using 7-Deaza-dGTP for droplet digital PCR quantification of TERT promoter mutations. Clin Chem 2018;64:745–7.

Fredriksson NJ, Elliott K, Filges S, Van den Eynden J, Stahlberg A, Larsson E. Recurrent promoter mutations in melanoma are defined by an extended context-specific mutational signature. PLoS Genet 2017;13:e1006773.

Fredriksson NJ, Ny L, Nilsson JA, Larsson E. Systematic analysis of noncoding somatic mutations and gene expression alterations across 14 tumor types. Nat Genet 2014;46:1258–63.

Griewank KG, Murali R, Puig-Butille JA, Schilling B, Livingstone E, Potrony M, et al. TERT promoter mutation status as an independent prognostic factor in cutaneous melanoma. J Natl Cancer Inst 2014;106(9).

Hayward NK, Wilmott JS, Waddell N, Johansson PA, Field MA, Nones K, et al. Whole-genome landscapes of major melanoma subtypes. Nature 2017;545(7653):175–80.

Heidenreich B, Nagore E, Rachakonda PS, Garcia-Casado Z, Requena C, Traves V, et al. Telomerase reverse transcriptase promoter mutations in primary cutaneous melanoma. Nat Commun 2014;5:3401.

Horn S, Figl A, Rachakonda PS, Fischer C, Sucker A, Gast A, et al. TERT promoter mutations in familial and sporadic melanoma. Science 2013;339(6122):959–61.

Huang FW, Hodis E, Xu MJ, Kryukov GV, Chin L, Garraway LA. Highly recurrent TERT promoter mutations in human melanoma. Science 2013;339(6122):957–9.

Lin WM, Luo S, Muzikansky A, Lobo AZ, Tanabe KK, Sober AJ, et al. Outcome of patients with de novo versus nevus-associated melanoma. J Am Acad Dermatol 2015;72:54–8.

Lu C, Zhang J, Nagahawatte P, Easton J, Lee S, Liu Z, et al. The genomic landscape of childhood and adolescent melanoma. J Invest Dermatol 2015;135:816–23.

Mao P, Brown AJ, Esaki S, Lockwood S, Poon GMK, Smerdon MJ, et al. ETS transcription factors induce a unique UV damage signature that drives recurrent mutagenesis in melanoma. Nat Commun 2018;9:2626.

Martincorena I, Campbell PJ. Somatic mutation in cancer and normal cells. Science 2015;349(6255):1483–9.

Melamed RD, Aydin IT, Rajan GS, Phelps R, Silvers DN, Emmett KJ, et al. Genomic characterization of dysplastic nevi unveils implications for diagnosis of melanoma. J Invest Dermatol 2017;137:905–9.

Melton C, Reuter JA, Spacek DV, Snyder M. Recurrent somatic mutations in regulatory regions of human cancer genomes. Nat Genet 2015;47:710–6.

Michaloglou C, Vredeveld LC, Soengas MS, Denoyelle C, Kuilman T, van der Horst CM, et al. BRAFE600-associated senescence-like cell cycle arrest of human naevi. Nature 2005;436(7051):720–4.

Nik-Zainal S, Kucab JE, Morganella S, Glodzik D, Alexandrov LB, Arlt VM, et al. The genome as a record of environmental exposure. Mutagenesis 2015;30:763–70.

Pampena R, Kyrgidis A, Lallas A, Moscarella E, Argenziano G, Longo C. A meta-analysis of nevus-associated melanoma: prevalence and practical implications. J Am Acad Dermatol 2017;77:938–45 e4.

Shain AH, Garrido M, Botton T, Talevich E, Yeh I, Sanborn JZ, et al. Exome sequencing of desmoplastic melanoma identifies recurrent NFKBIE promoter mutations and diverse activating mutations in the MAPK pathway. Nat Genet 2015a;47:1194–9.

Shain AH, Joseph NM, Yu R, Benhamida J, Liu S, Prow T, et al. Genomic and transcriptomic analysis reveals incremental disruption of key signaling pathways during melanoma evolution. Cancer Cell 2018;34:45–55 e4.

Shain AH, Yeh I, Kovalyshyn I, Sriharan A, Talevich E, Gagnon A, et al. The genetic evolution of melanoma from precursor lesions. N Engl J Med 2015b;373:1926–36.

Stark MS, Tan JM, Tom L, Jagirdar K, Lambie D, Schaider H, et al. Whole-exome sequencing of acquired nevi identifies mechanisms for development and maintenance of benign neoplasms. J Invest Dermatol 2018;138:1636–44.

The Cancer Genome Atlas Network. Genomic classification of cutaneous melanoma. Cell 2015;161:1681–96.

Tsao H, Bevona C, Goggins W, Quinn T. The transformation rate of moles (melanocytic nevi) into cutaneous melanoma: a population-based estimate. Arch Dermatol 2003;139:282–8.

Tsao SC, Weiss J, Hudson C, Christophi C, Cebon J, Behren A, et al. Monitoring response to therapy in melanoma by quantifying circulating tumour DNA with droplet digital PCR for BRAF and NRAS mutations. Sci Rep 2015;5:11198.

Vinagre J, Almeida A, Populo H, Batista R, Lyra J, Pinto V, et al. Frequency of TERT promoter mutations in human cancers. Nat Commun 2013;4:2185.

Weinhold N, Jacobsen A, Schultz N, Sander C, Lee W. Genome-wide analysis of noncoding regulatory mutations in cancer. Nat Genet 2014;46:1160–5.

Wilmott JS, Field MA, Johansson PA, Kakavand H, Shang P, De Paoli-Iseppi R, et al. Tumour procurement, DNA extraction, coverage analysis and optimisation of mutation-detection algorithms for human melanoma genomes. Pathology 2015;47:683–93.

Zhang T, Dutton-Regester K, Brown KM, Hayward NK. The genomic landscape of cutaneous melanoma. Pigment Cell Melanoma Res 2016;29:266–83.